

Dark photon manifestation in the tripletlike QED processes

$$\gamma + \ell_i \rightarrow \ell_j^+ \ell_j^- + \ell_i, \quad i \neq j, \quad i = e, \mu, \quad j = e, \mu, \tau$$

G. I. Gakh*

*National Science Centre, Kharkov Institute of Physics and Technology,
Akademicheskaya 1, and V. N. Karazin Kharkov National University,
Department of Physics and Technology,
31 Kurchatov, 61108 Kharkov, Ukraine*

M.I. Konchatnij[†] and N.P. Merenkov[‡]

*National Science Centre, Kharkov Institute of Physics and Technology,
Akademicheskaya 1, and V. N. Karazin Kharkov National University,
Dept. of Physics and Technology, 31 Kurchatov, 61108 Kharkov, Ukraine*

E. Tomasi-Gustafsson[§]

IRFU, CEA, Université Paris-Saclay, 91191 Gif-sur-Yvette, France

Abstract

The tripletlike QED processes $\gamma + \ell_i \rightarrow \ell_j^+ \ell_j^- + \ell_i$ with $i \neq j$, and $i = e, \mu$, $j = e, \mu, \tau$ has been investigated as the reactions where a dark photon, A' , is produced as a virtual state with subsequent decay into a $\ell_j^+ \ell_j^-$ pair. This effect arises due to the so-called kinetic mixing and is characterized by a small parameter ϵ describing the coupling strength relative to the electric charge e . In these processes, the dark photon appears as a resonance with Breit-Wigner propagator in the $\ell_j^+ \ell_j^-$ system. The distributions over the invariant mass of the produced $\ell_j^+ \ell_j^-$ pair is calculated and the value of the parameter ϵ , as a function of the dark photon mass, is estimated for a given number of measured events in the specific experimental conditions. Assuming a standard deviation of $\sigma = 2$ (corresponding to ≈ 95 % confidence limit) and a number of measured events equal to 10^4 , we obtain the following limits for the parameter space of the dark photon: $\epsilon^2 \leq 10^{-7}$ ($\gamma + \mu^- \rightarrow e^+ + e^- + \mu^-$) and $\epsilon^2 \leq 10^{-7} \div 6 \times 10^{-8}$ ($\gamma + e^- \rightarrow \mu^+ + \mu^- + e^-$) in the A' mass region $520 < m_{A'} < 980$ MeV. In the mass region $30 < M_{A'} < 400$ MeV we obtain $\epsilon^2 \leq 10^{-7}$ ($\gamma + \mu^- \rightarrow e^+ + e^- + \mu^-$).

PACS numbers: 13.40-f,13.40.Gp,13.88+e

* gakh@kipt.kharkov.ua

† konchatnij@kipt.kharkov.ua

‡ merenkov@@kipt.kharkov.ua

§ egle.tomasi@cea.fr

I. INTRODUCTION

Cosmological and astrophysical measurements give evidence of the existence of dark matter. Its nature and interaction are unknown today. The recent experimental discoveries, such as neutrino oscillations (that imply massive neutrinos [1]), and the discrepancy between the Standard Model (SM) prediction and the measured value of the anomalous magnetic moment of the muon [2], as well as recent measurements of flavor-changing processes in B meson decays (showing tensions with the SM predictions [3]), lead one to consider physics beyond the SM (see the reviews [4–7]). The extension of the SM includes various models predicting a number of new particles. The so-called dark photon (DP), A' , is one of the possible new particles. It is a massive vector boson that can mix with the ordinary photon via "kinetic mixing" [8]. Its mass and interaction strength are not predicted unambiguously by the theory, since DPs can arise via different mechanisms. Various theoretically motivated regions of the DP mass are given in Ref. [4]. A DP with mass larger than 1 MeV can be produced in electron (proton) fixed-target experiments or at hadron or electron-positron colliders (see the references in the review [4]). The properties of a DP with a mass in the range eV - keV can be determined using astrophysical data.

A number of experiments searching for DPs are carried out or planned in various laboratories. Using APEX test run data obtained at the Jefferson Laboratory [9, 10], the DP was searched in electron-nucleus fixed-target scattering in the mass range 175–250 MeV. The DarkLight Collaboration [11] (JLab) studied the prospects for detecting a light boson with mass $m_X \leq 100$ MeV in electron-proton scattering. The produced A' decays to an e^+e^- pair leading to the $e^-pe^+e^-$ final state. An exclusion limit for the electromagnetic production of a light A' decaying to e^+e^- was determined by the A1 Collaboration at the Mainz Microtron MAMI ([12] using electron scattering from a heavy nucleus. The Heavy Photon Search (HPS) experiment [13] searches for an electroproduced DP using an electron beam provided by the Continuous Electron Beam Accelerator Facility accelerator at JLab. HPS looks for DPs through two distinct methods - the search of a resonance in the e^+e^- invariant mass distribution above the large QED background (large DP-SM particles coupling region) - and the search of a displaced vertex for long-lived DPs (small coupling region).

The manifestation of DPs is also searched for in the decay of known particles. The authors of Ref. [14] have studied the radiative pion decay, $\pi^+ \rightarrow e^+\nu\gamma$. The measurements

were performed at the π E1 channel of the Paul Scherrer Institute, Switzerland. The DP was also searched for in the decay of π^0 -mesons ($\pi^0 \rightarrow \gamma A' \rightarrow \gamma e^+ e^-$) produced in proton-nuclei collisions at the Heavy Ion Accelerator Facility (China) [15]. The decay of π^0 -meson was the tool to search for the DP also in the experiment at WASA-at-COSY(Jülich, Germany) (π^0 -mesons were produced in the reaction $pp \rightarrow pp\pi^0$) [16] and at CERN, where π^0 -mesons were produced in the decay of K -mesons, $K^\pm \rightarrow \pi^\pm \pi^0$ [17].

The search for a DP signal in inclusive dielectron spectra in proton-induced reactions on either a liquid hydrogen target or on a nuclear target was performed at the GSI in Darmstadt [18]. An upper limit on the DP mixing parameter in the mass range $m(A') = 0.02 - 0.6 \text{ GeV}/c^2$ was established. The constraints on the DP parameters from the data collected in experiments with electron beams were summarized in Ref. [19]. At JLab, it was demonstrated that electron-beam fixed-target experiments would have a powerful discovery potential for DPs in the MeV-GeV mass range [20]. Reference [21] describes some of the main dark sector searches performed by the Belle II experiment at the SuperKEKB energy-asymmetric e^+e^- collider (a substantial upgrade of the B factory facility at the Japanese KEK laboratory). The design luminosity of the machine is $8 \times 10^{35} \text{ cm}^{-2}\text{s}^{-1}$. At Belle II, the DP is searched for in the reaction $e^+e^- \rightarrow \gamma_{ISR} A'$, with subsequent decays of the DP to dark matter $A' \rightarrow \chi\bar{\chi}$ (ISR stays for initial state radiation). The main backgrounds come from QED processes such as $e^+e^- \rightarrow e^+e^-\gamma(\gamma)$ and $e^+e^- \rightarrow \gamma\gamma(\gamma)$. Preliminary studies have been performed and the sensitivity to the kinetic mixing parameter strength is given. With a small integrated luminosity a very competitive measurement is possible, especially in the region for $M_{A'} > \text{few times } 10 \text{ MeV}/c^2$ where the BABAR experiment starts dominating in terms of sensitivity [22]. An experiment to search for A' was proposed at VEPP-3 (electron-positron collider) (Russia) [23]. The search method is based on the missing mass spectrum in the reaction $e^+e^- \rightarrow \gamma A'$. At the future CEPC experiment (China) running at $\sqrt{s} = 91.2 \text{ GeV}$ it is possible for CEPC to perform a decisive measurement on a DP in the mass region $20 \text{ GeV} < m_{A'} < 60 \text{ GeV}$, in about 3 months of operation [24]. $\sqrt{s} = 240 \text{ GeV}$ is also achievable.

DP formation in various reactions was investigated theoretically in a number of papers. Bjorken *et al.* [25] considered several possible experimental setups for experiments aimed at the search for A' in the most probable range of masses from a few MeV to several GeV and confirmed that the experiments at a fixed target perfectly suit for the discovery of DPs in

this interval of masses. DP production in the process of electron scattering on a proton or on heavy nuclei has been investigated in Ref. [26] (Ref. [27]) for the experimental conditions of the MAMI (JLab) experiment [12] (Ref. [10]). The authors of Ref. [28] proposed to use rare leptonic decays of kaons and pions $K^+(\pi^+) \rightarrow \mu^+\nu_\mu e^+e^-$ to study the light DP (with a mass of about 10 MeV). The constraints on DPs in the 0.01-100 keV mass range are derived in Ref. [29] (the indirect constraints following from $A' \rightarrow 3\gamma$ decay are also revisited). The proposal to search for light DPs using the Compton-like process, $\gamma e \rightarrow A'e$, in a nuclear reactor was suggested in Ref. [30]. This suggestion was developed in Ref. [31], where the constraints on some DP parameters were determined using the experimental data obtained at the Taiwan EXperiment On Neutrino reactor (TEXONO). Some results on the phenomenology of the DP in the mass range of a few MeV to GeV have been presented in Ref. [32], where $g - 2$ of muons and electrons together with other precision QED data, as well as radiative decays of strange particles were analyzed.

The process of the triplet photoproduction on a free electron, $\gamma + e^- \rightarrow e^+ + e^- + e^-$, in which A' can be formed as an intermediate state with subsequent decay into an e^+e^- pair was investigated in Ref. [33]. The advantage of this process is that the background is a purely QED process $\gamma + e^- \rightarrow e^+ + e^- + e^-$, which can be calculated with the required accuracy. The analysis was done by taking into account the identity of the final electrons. The constraints on parameter ϵ depending on the DP mass and the statistics (number) of events were obtained with a special method of gathering events where the invariant mass of one e^+e^- pair remains fixed while the other pair is scanned.

The search for DPs produced at e^+e^- colliders in the forward region was considered in Ref. [34]. An additional detector set around BESIII can probe the DP coupling parameter ϵ down to 2×10^{-4} , whereas at Belle-II, it would have a higher sensitivity down to 2×10^{-5} .

It should be mentioned that the constraints on the DP parameters can be obtained using astrophysical data and that the astrophysical constraints on the DP with masses in the range $M_{A'} \leq (\text{eV-keV})$ are stronger than laboratory constraints (see, for example, Refs. [35, 36]). The calculation of the cooling rates for the Sun gives the following constraint on the DP parameter space ($m_{A'} < 0.1 \text{ eV}$) [37]:

$$\epsilon \times \frac{m_{A'}}{\text{eV}} < 1.4 \times 10^{-11}.$$

The magnetometer data from *Voyager* [38] probes DPs in the 10^{-24} to 10^{-19} eV mass range.

Values of the coupling parameter ϵ as low as 3×10^{-5} for the highest masses were excluded. The proposed search for DPs using the Alpha Magnetic Spectrometer [39] has a potential discovery for mass $m_{A'} \sim \mathcal{O}(100)$ MeV and kinetic mixing parameters $10^{-10} \leq \epsilon \leq 10^{-8}$. More information about DP (and dark matter) searches in astrophysical experiments can be found in Ref. [40].

In this work, we suggest a possible way to detect the DP signal through the reaction $\gamma + \ell_i \rightarrow \ell_j^+ \ell_j^- + \ell_i$ (ℓ is a lepton), where a few tens MeV photon collides with a high-energy electron or muon beam. The advantage of this reaction, as compared with the reaction $\gamma + e^- \rightarrow e^+ + e^- + e^-$ considered in Ref. [33], is that there are no identical particles in the final state. So, the analysis of the experimental results is simpler. We calculate the distributions over the invariant mass of the produced $\ell_j^+ \ell_j^-$ - pair and search for the kinematical region where the Compton-type diagram contribution is not suppressed with respect to the Borsellino ones. The distributions for the proposed reaction are more interesting (corresponding to a larger number of events) due to the increased phase space, since it is not necessary to fix the parameters of the second pair. We estimated the value of the parameter ϵ as a function of the DP mass, for a given number of measured events.

This work is organized in the following way: Section II contains the formalism for calculating the distribution over the invariant mass of the produced lepton pair. The kinematics of the proposed reaction is briefly considered in Sec. IIA. The calculation of the distribution over the invariant mass of the produced lepton pair, which is caused by the QED mechanism, is given in Sec. IIB. Section III is devoted to the analysis of the DP effects in the proposed reaction. Here we estimate the coupling constant ϵ as a function of the DP mass and the number of the measured events. The analytic form for the double differential cross section is given in the Appendix. Finally, in Sec. IV we summarize our conclusions.

II. FORMALISM

We assume that the DP can manifest itself as some intermediate state with the photon quantum numbers that decays into a $\ell_j^+ \ell_j^-$ pair. In such a case, the process

$$\gamma(k) + \ell_i^-(p) \rightarrow \ell_j^+(p_3) + \ell_j^-(p_1) + \ell_i^-(p_2), \quad (1)$$

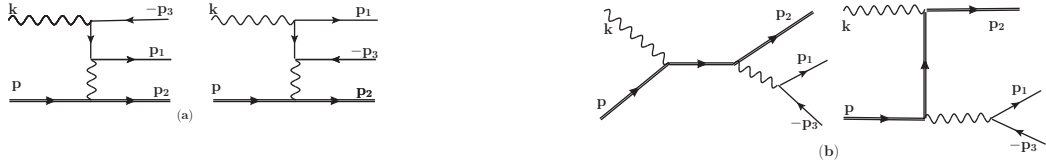


FIG. 1. The Feynman diagrams for the process (1). Diagrams (a) are called the Borsellino diagrams, and diagrams (b) are the Compton-type diagrams.

in which a high-energy electron or muon interacts with a few tens MeV photon, can be used, in principle, to probe the A' signal in a wide range of A' masses, from a few MeV up to 10 GeV.

We suggest to scan the differential cross section over the $\ell_j^+ \ell_j^-$ invariant mass, $s_1 = (p_3 + p_1)^2$. The background, due to a pure QED mechanism, exceeds essentially the DP effect and has to be calculated with high accuracy. In the lowest approximation, the QED amplitude of the process (1) is given by the four diagrams shown in Fig. 1. The DP effect is calculated as a modification of the photon propagator in the single-photon (the Compton type) diagrams Fig. 1(b).

The applied method is the following: We calculate first the double differential cross section over the invariant variables s_1 and $u = (k - p_2)^2$. Next, we find the kinematical region, in terms of these variables, where the single-photon amplitudes give a comparable or larger contribution with respect to the double-photon amplitudes of the Borsellino diagrams in Fig. 1(a). This region can be delimited by excluding the large $|u|$ values with appropriate cuts. Then, we perform an integration over the variable u in this restricted region and

include the effect due to the DP contribution.

A. Kinematics

To describe the process (1) we introduce the following set of invariant variables [41]:

$$\begin{aligned}
s &= (k+p)^2 = (p_1+p_2+p_3)^2, \quad s_1 = (p_1+p_3)^2 = (k+p-p_2)^2, \\
s_2 &= (p_2+p_3)^2 = (k+p-p_1)^2, \\
t_1 &= (k-p_1)^2 = (p_2+p_3-p)^2, \quad t_2 = (p-p_2)^2 = (p_1+p_3-k)^2.
\end{aligned} \tag{2}$$

In terms of these variables, we have:

$$\begin{aligned}
2(kp_2) &= s - s_1 + t_2 - M^2, \quad 2(kp) = s - M^2, \quad 2(kp_1) = m^2 - t_1, \\
2(kp_3) &= s_1 + t_1 - t_2 - m^2, \quad u = 2M^2 - s + s_1 - t_2, \\
2(pp_1) &= s - s_2 + t_1, \quad 2(pp_2) = 2M^2 - t_2, \quad 2(pp_3) = s_2 - t_1 + t_2 - M^2, \\
2(p_1p_3) &= s_1 - 2m^2, \quad 2(p_2p_3) = s_2 - M^2 - m^2, \quad 2(p_1p_2) = s - s_1 - s_2 + m^2,
\end{aligned} \tag{3}$$

where M (m) is the mass of the initial (created) lepton.

For back-to-back events azimuthal symmetry applies and the phase space of the final particles can be written as [41]:

$$dR_3 = \frac{d^3p_1}{2E_1} \frac{d^3p_2}{2E_2} \frac{d^3p_3}{2E_3} \delta(k+p-p_1-p_2-p_3) = \frac{\pi}{16(s-M^2)} \frac{dt_1 dt_2 ds_1 ds_2}{\sqrt{-\Delta}}, \tag{4}$$

where Δ is the Gramian determinant. The limits of integration are defined by the condition of the positiveness of $(-\Delta)$. In Ref. [33] these limits have been obtained for the triplet production process where the masses of all leptons are equal. Similarly, we obtain for the considered reactions

$$t_{1-} < t_1 < t_{1+}, \quad t_{1\pm} = \frac{A \pm 2\sqrt{B}}{(s-s_1)^2 - 2(s+s_1)M^2 + M^4}, \tag{5}$$

where

$$\begin{aligned}
A &= \left\{ -M^4 s_1 + s_1 s_2 (s_1 - t_2) + s^2 t_2 + M^2 [s_1^2 + s_1 s_2 + s(s_1 - t_2) + s_2 t_2] - \right. \\
&\quad \left. s [s_2 t_2 + s_1 (s_2 + t_2)] + m^2 [M^4 + s(s-s_1) + (s+s_1)t_2 - M^2(2s+3s_1+t_2)] \right\}, \\
B &= [s t_2 (s-s_1+t_2) + M^2 (s_1^2 - 2s t_2 - s_1 t_2) + M^4 t_2] \times [m^2 M^4 + m^4 s_1 - m^2 M^2 (2s+s_1) + \\
&\quad m^2 (s^2 - s s_1 - 2s_1 s_2) + M^2 s_1 (s-s_2) + s_1 s_2 (-s+s_1+s_2)].
\end{aligned}$$

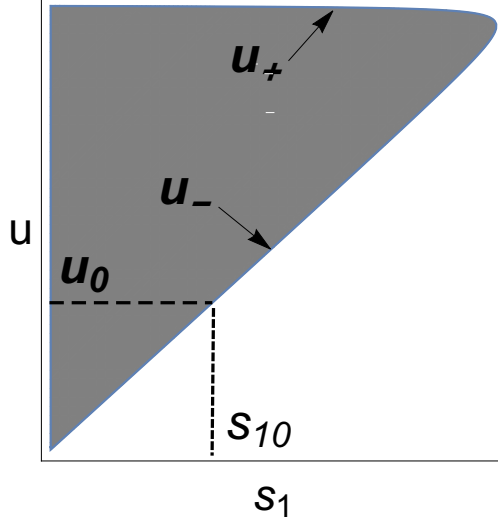


FIG. 2. Kinematical region for (s_1, u) . The quantity s_{10} is the solution of the equation $u_0 = u_-$, where u_0 is the negative cut parameter.

At fixed s_1 and t_2 , we have $s_{2-} < s_2 < s_{2+}$ where

$$s_{2\pm} = \frac{2m^2 + M^2 + s - s_1 \pm \lambda_1 \sqrt{1 - \frac{4m^2}{s_1}}}{2}, \quad \lambda_1 = \sqrt{(s - s_1)^2 - 2M^2(s + s_1) + M^4}. \quad (6)$$

The corresponding range for t_2 , $t_{2-} < t_2 < t_{2+}$ and for s_1 , $4m^2 < s_1 < (\sqrt{s} - M)^2$, is limited by the curves

$$t_{2\pm} = \frac{1}{2s} [C \pm \lambda_1(M^2 - s)], \quad C = s_1(s + M^2) - (s - M^2)^2. \quad (7)$$

Furthermore, it is preferred to use the variable u instead of t_2 because one of the Compton-type diagrams has a pole behavior precisely in the u channel. The kinematical region (s_1, u) is shown in Fig. 2, where:

$$u_{\pm} = \frac{1}{2s} [\bar{C} \pm \lambda_1(s - M^2)], \quad \bar{C} = M^4 + M^2(2s - s_1) - s(s - s_1). \quad (8)$$

B. Calculation of the QED cross section

In the case of unpolarized particles, we have to average over (to sum over) the polarization states of the initial (final) particles. The differential cross section can be written in the form

$$d\sigma = \frac{1}{4} \frac{e^6}{4(kp)(2\pi)^5} \sum_{pol} |M|^2 dR_3, \quad (9)$$

where M is the matrix element of the process (1):

$$\sum_{pol} |M|^2 = |M_b|^2 + |M_c|^2 + 2\mathcal{R}[M_b M_c^*], \quad (10)$$

and the index b (c) corresponds to the Borsellino (the Compton-type) diagrams.

The double differential cross section, as a function of the variables s_1 and t_2 [or the (s_1, t_2) distribution], is

$$\frac{d\sigma}{ds_1 dt_2} = \frac{\alpha^3}{64\pi(s-M^2)^2} \int \int \frac{ds_2 dt_1}{\sqrt{-\Delta}} \sum_{pol} |M|^2. \quad (11)$$

The calculation of the matrix element squared (10) gives:

$$\begin{aligned} |M_b|^2 = & \frac{8}{t_2^2} \left\{ \frac{8d^2 m^2}{d_3^2} + t_2^2 \left[\left(\frac{1}{d_3^2} + \frac{1}{d_1^2} \right) m^2 - \frac{2M^2}{d_1 d_3} - \frac{2}{d_3} \left(\frac{d}{d_1} + 1 \right) \right] + \right. \\ & 8(\text{pp}_3)^2 \left[\left(\frac{1}{d_3} + \frac{1}{d_1} \right)^2 m^2 - \frac{t_2}{d_1 d_3} \right] + \\ & 4(\text{pp}_3) \left[t_2 \left(-m^2 \left(\frac{1}{d_3} + \frac{1}{d_1} \right)^2 - \frac{1}{d_1} + \frac{2d}{d_1 d_3} + \frac{1}{d_3} \right) - \frac{4d}{d_3} \left(\frac{1}{d_3} + \frac{1}{d_1} \right) m^2 + \frac{t_2^2}{d_1 d_3} \right] + \\ & t_2 \left[2 \left(\frac{1}{d_3} + \frac{1}{d_1} \right)^2 m^4 + 2 \left(\frac{1}{d_3} + \frac{1}{d_1} \right)^2 m^2 M^2 + 4 \left(\frac{1}{d_3} + \frac{1}{d_1} \right) \left(\frac{d}{d_3} - 1 \right) m^2 - \right. \\ & \left. \left. 4 \left(\frac{1}{d_3} + \frac{1}{d_1} \right) M^2 - 2 \left(\frac{d_1}{d_3} + \frac{2d}{d_1} \left(\frac{d}{d_3} - 1 \right) + \frac{d_3}{d_1} \right) \right] - 4 \left(\frac{d_1}{d_3} + \frac{d_3}{d_1} \right) M^2 - \frac{t_2^3}{d_1 d_3} \right\}, \end{aligned}$$

$$|M_c|^2 = |M_b|^2(p \leftrightarrow -p_3, p_1 \leftrightarrow p_2, m \leftrightarrow M), \quad d_i = (kp_i).$$

On the level of the full differential cross section, the interference of M_c and M_b contributes also, but in the experimental setup considered in this paper, where only the scattered ℓ_i lepton is recorded, it vanishes due to the Furry theorem [42].

Introducing the short notation:

$$\frac{\pi}{64(s-M^2)} \int_{s_{2-}}^{s_{2+}} ds_2 \int_{t_{1-}}^{t_{1+}} dt_1 \frac{W}{\sqrt{-\Delta}} \equiv \widehat{W},$$

and applying the relation (3) between the variables t_2 and u , we have

$$\begin{aligned} \widehat{|M_c|^2} = & \frac{2\pi^2 \sqrt{1 - \frac{4m^2}{s_1}} (2m^2 + s_1)}{3(M^2 - s)^2 s_1^3 (M^2 - u)} \times \\ & \left\{ -4M^6 + (s - s_1 + u)(5M^4 - 2s_1^2 + su) - M^2 [s^2 - 4s_1^2 + s_1 u + u^2 + s(s_1 + 6u)] \right\}, \end{aligned} \quad (12)$$

$$\begin{aligned}
\overbrace{|M_b|^2} &= \frac{4\pi^2}{(M^2 - s)(2M^2 - s + s_1 - u)^2} \times \\
&\left\{ \ln \left(\frac{\sqrt{s_1 - 4m^2} + \sqrt{s_1}}{2m} \right) \left[\frac{4s_1[s_1^2 - 2m^2(2m^2 - 3s_1)](M^2 - s)^2}{(-2M^2 + s + u)^4} - \right. \right. \\
&\frac{4(M^2 - s)[2m^2(2m^2(M^2 - s - s_1) + s_1(-5M^2 + 5s + 3s_1)) + s_1^2(-2M^2 + 2s + s_1)]}{(2M^2 - s - u)^3} - \\
&\frac{2[-4m^4 + m^2(-8M^2 + 8s + 2s_1) + (M^2 - s)^2 + s_1(-M^2 + 3s + 2s_1)]}{-2M^2 + s + u} + \\
&\frac{1}{(-2M^2 + s + u)^2} 2[2m^2(4(M^2 - s)^2 + s_1(10s + s_1 - 8M^2) - 2m^2(2s + s_1)) + \\
&s_1(3(M^2 - s)^2 + s_1(4s + s_1 - 2M^2))] + 2M^2 + s + 3s_1 - u \left. \right\} - \\
&\sqrt{1 - \frac{4m^2}{s_1}} \left[- \frac{4(M^2 - s)[m^2s_1(M^2 - s - s_1) + 2s_1^2(2M^2 - 2s - s_1)]}{(-2M^2 + s + u)^3} + \right. \\
&\frac{4s_1^2(M^2 - s)^2(m^2 + 2s_1)}{(-2M^2 + s + u)^4} + \\
&\frac{s_1[2m^2(2s + s_1) + 9(M^2 - s)^2 + 2s_1(-6M^2 + 8s + s_1)]}{(-2M^2 + s + u)^2} - \\
&\left. \frac{s_1(2m^2 - 5M^2 + 9s + 4s_1) + (M^2 - s)^2}{-2M^2 + s + u} + \frac{1}{2}(2M^2 + s + 5s_1 - u) \right] \left. \right\}. \quad (13)
\end{aligned}$$

Following Eq. (11) and the definition of the quantity \overbrace{W} , the double differential cross section can be written as

$$\frac{d\sigma}{ds_1 du} = \frac{\alpha^3}{\pi^2(s - M^2)} \sum_{pol} \overbrace{|M|^2}, \quad (14)$$

where $\sum_{pol} |M|^2$ is defined by Eq. (10). To measure the differential cross section $d\sigma/(ds_1 du)$, it is sufficient to detect the final muon 4-momenta.

The integration of the double differential cross section (14) with respect to the variable u in the limits $u_- < u < u_+$ gives

$$\begin{aligned}
\frac{d\sigma_c}{ds_1} &= \frac{\alpha^3 \sqrt{1 - \frac{4m^2}{s_1}} (2m^2 + s_1)}{3\pi s_1^2 (s - M^2)^3} \left\{ \frac{\lambda_1 [M^6 - M^4(s + s_1) + M^2s(15s + 2s_1) + s^2(s + 7s_1)]}{2s^2} - \right. \\
&\left. [3M^4 + M^2(6s - 2s_1) - s^2 + 2(s - s_1)s_1] \ln \left[\frac{(M^2 + s - s_1 + \lambda_1)^2}{4M^2s} \right] \right\}, \quad (15)
\end{aligned}$$

$$\begin{aligned}
\frac{d\sigma_b}{ds_1} = \frac{2\alpha^3}{\pi(s-M^2)} & \left\{ \frac{2\lambda_1 \sqrt{1 - \frac{4m^2}{s_1}}}{3s_1^3(M^2 - s)^2} \right. & (16) \\
& \left[m^2[17(M^2 - s)^2 + 2s_1(4M^2 - 2s + s_1)] + s_1[7(M^2 - s)^2 + s_1(4M^2 - 2s + s_1)] \right] + \\
& \frac{1}{s_1^4(s - M^2)} \left[s_1 \sqrt{1 - \frac{4m^2}{s_1}} [2m^2[2(M^2 - s)^2 + s_1(6M^2 - 2s + s_1)] \right. \\
& + s_1[(M^2 - s)^2 + s_1(5M^2 - s)] + 2[4m^4[2(M^2 - s)^2 + s_1(6M^2 - 2s + s_1)] - \\
& - 2m^2 s_1[2(M^2 - s)^2 + s_1(6M^2 - 2s + s_1)] - \\
& \left. s_1^2[(M^2 - s)^2 + s_1(3M^2 - s)] \right] \ln \left(\frac{\sqrt{s_1 - 4m^2} + \sqrt{s_1}}{2m} \right) \Big] \times \\
& \ln \left(\frac{(\lambda_1 - M^2 + s + s_1)^2}{4s s_1} \right) - \\
& \frac{2\lambda_1}{3s_1^4(M^2 - s)^2} [-4m^4[17(M^2 - s)^2 + 2s_1(4M^2 - 2s + s_1)] + \\
& 6m^2 s_1(M^2 - s)(7M^2 - 7s + 2s_1) + \\
& s_1^2[8(M^2 - s)^2 + s_1(5M^2 - s + 2s_1)]] \times \ln \left(\frac{\sqrt{s_1 - 4m^2} + \sqrt{s_1}}{2m} \right) + \\
& \frac{1}{2s_1^4(s - M^2)} \left[s_1 \sqrt{1 - \frac{4m^2}{s_1}} [4m^2[2(M^2 - s)^2 + s_1(6M^2 - 2s + s_1)] + \right. \\
& + s_1[2(M^2 - s)^2 + s_1(10M^2 - 2s + s_1)]] + \\
& 2(8m^4 - 4m^2 s_1 - s_1^2)[2(M^2 - s)^2 + s_1(6M^2 - 2s + s_1)] \times \\
& \left. \ln \left(\frac{\sqrt{s_1 - 4m^2} + \sqrt{s_1}}{2m} \right) \right] \ln \left[\frac{[M^4 + \lambda_1(M^2 - s) - M^2(2s + s_1) + s(s - s_1)]^2}{4M^2 s s_1^2} \right] \Big\} .
\end{aligned}$$

We can also write a more complicated analytical expression for $d\sigma/ds_1$ accounting for the restriction on the variable u . The corresponding result is given in the Appendix.

In the limiting case $s \gg (s_1, M^2) \gg m^2$, which applies for electron-positron pair production, these expressions are essentially simplified, namely

$$\begin{aligned}
\frac{d\sigma_c}{ds_1} &= \frac{\alpha^3}{3\pi s s_1} \left[\frac{1}{2} + \frac{17M^2 + 2s_1}{2s} + \left(1 - \frac{3M^2 + 2s_1}{s} \right) \ln \frac{s}{M^2} \right], \\
\frac{d\sigma_b}{ds_1} &= \frac{2\alpha^3}{\pi s_1^2} \left\{ \ln \frac{s_1}{m^2} \ln \frac{s^2}{s_1 M^2} - \frac{8}{3} \ln \frac{s_1}{m^2} - \ln \frac{s^2}{s_1 M^2} + \frac{14}{3} + \right. \\
& \left. \frac{1}{s} \left[-s_1 \ln \frac{s_1}{m^2} \ln \frac{s^2}{s_1 M^2} + (s_1 - 2M^2) \ln \frac{s_1}{m^2} + s_1 \ln \frac{s^2}{s_1 M^2} - 4s_1 + 2M^2 \right] \right\} .
\end{aligned}$$

Eqs. (15) and (16) hold for particles with arbitrary masses. They can be applied to the

reactions:

$$\gamma + e^- \rightarrow \mu^+ \mu^- + e^-, \quad \gamma + e^- \rightarrow \tau^+ \tau^- + e^-, \quad \gamma + \mu^- \rightarrow \tau^+ \tau^- + \mu^-,$$

and the asymptotic formulas, in the limit $s \gg (s_1, m^2) \gg M^2$, valid for muon pair production, become:

$$\begin{aligned} \frac{d\sigma_c}{ds_1} &= \frac{\alpha^3}{6\pi s s_1} (2+y) \sqrt{1-y} \left[\frac{1}{2} + x_1 + (1-2x_1) \ln \frac{s}{M^2} \right], \quad x_1 = \frac{s_1}{s}, \quad y = \frac{4m^2}{s_1}, \\ \frac{d\sigma_b}{ds_1} &= \frac{2\alpha^3}{\pi s_1^2} \left\{ \left[(2+2y-y^2)L - (1+y)\sqrt{1-y} \right] (1-x_1) \ln \frac{s^2}{M^2 s_1} + \right. \\ &\quad \left. \left[\frac{17}{6}y^2 - 7y - \frac{16}{3} + x_1 \left(2 + 5y - \frac{3}{2}y^2 \right) \right] L + \sqrt{1-y} \left[\frac{14}{3} + \frac{17}{6}y - x_1 \left(4 + \frac{3}{2}y \right) \right] \right\}, \\ L &= \ln \frac{\sqrt{s_1} + \sqrt{s_1 - 4m^2}}{2m}. \end{aligned}$$

III. ANALYSIS OF THE DARK PHOTON SIGNAL

We have to estimate first the QED background in order to find the kinematical conditions where the cross section $d\sigma_c/ds_1$ exceeds $d\sigma_b/ds_1$, because in our work, the DP signal is related to a modification of the Compton-type diagrams. We perform the following calculations for e^+e^- pair creation.

It is well known that at photon energies larger than 10 MeV, the main contribution to the cross section of the tripletlike processes arises from the Borsellino diagrams due to the events at small values of t_2 [43].

In Fig. 3, we show : (a) the differential cross section, i.e., the sum of (15) and (16) contributions as a function of the dimensionless variable $x_1 = s_1/s$ at fixed s , and (b) the ratio of the Compton-type diagrams contribution to the Borsellino ones as a function of s_1 ,

$$R_b^c = \frac{d\sigma_c}{d\sigma_b},$$

at different colliding energies: $s = 6, 30, 60 \text{ GeV}^2$, provided that the whole kinematical region (s_1, u) is allowed. We see that in a wide, physically interesting range of variable s_1 , the quantity $R_b^c(s_1)$ is rather small (does not exceed $2 \cdot 10^{-2}$) and it is obvious that, in the case of the nonlimited phase space, the Borsellino contribution leads to a very large QED background for searching for a small DP signal which modifies the Compton-type contribution only.

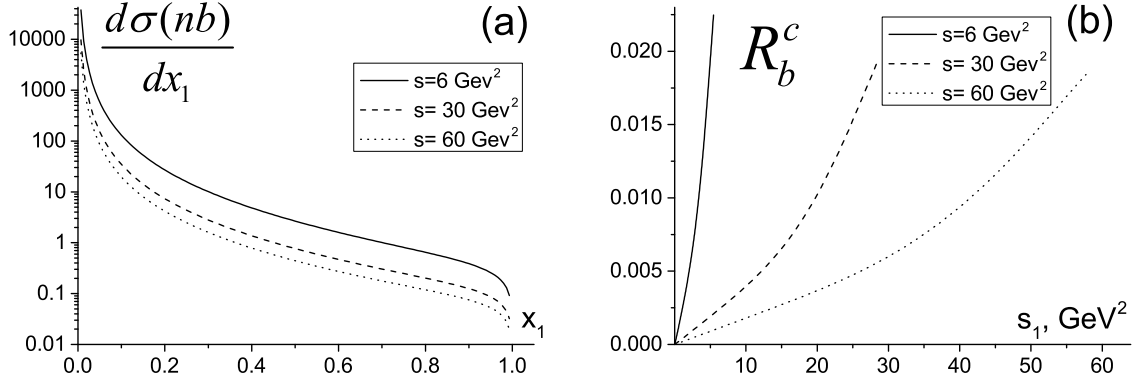


FIG. 3. (a) Differential cross section of the process $\gamma + \mu^- \rightarrow e^+ e^- + \mu^-$, as a function of $x_1 = s_1/s$ for fixed values of the variable s , calculated with Eqs. (15) and (16); (b) Ratio of the contributions to the cross section of the Compton-type diagrams to the Borsellino ones as a function of the e^+e^- invariant mass squared,

To find the kinematical region where the signal over background ratio is maximized, we analyze the double (s_1, u) distribution separately for the Compton and Borsellino contributions, using relations (12) and (13), and the results are presented in Fig. 4, where we plot the corresponding double differential cross sections and from which one can easily determine the regions where the Compton contribution exceeds the Borsellino one. We see that the contribution due to the Compton-type diagrams increases with decrease of both variables, s_1 and $|u|$, whereas the contribution of the Borsellino diagrams indicates just the opposite behaviour. Since we have to scan s_1 -distribution, we can restrict the (s_1, u) region by cutting the large values of $|u|$ in order to reach our goal.

As one can see from the curves in Fig. 4, there is a large region of variables u and s_1 where the Compton contribution exceeds the Borsellino one, and it indicates that measurements should be preferentially performed in this region to detect the DP signal in form of a resonance in the single-photon intermediate state. The corresponding regions for the different reactions are shown in Fig. 5.

To reduce the Borsellino contribution, we suggest to remove the events with small values of the variable $|t_2|$ (or with large values of $|u|$) by the kinematical cut:

$$u > u_0, \quad (17)$$

where u_0 is a negative parameter that may take different values in the numerical calculations

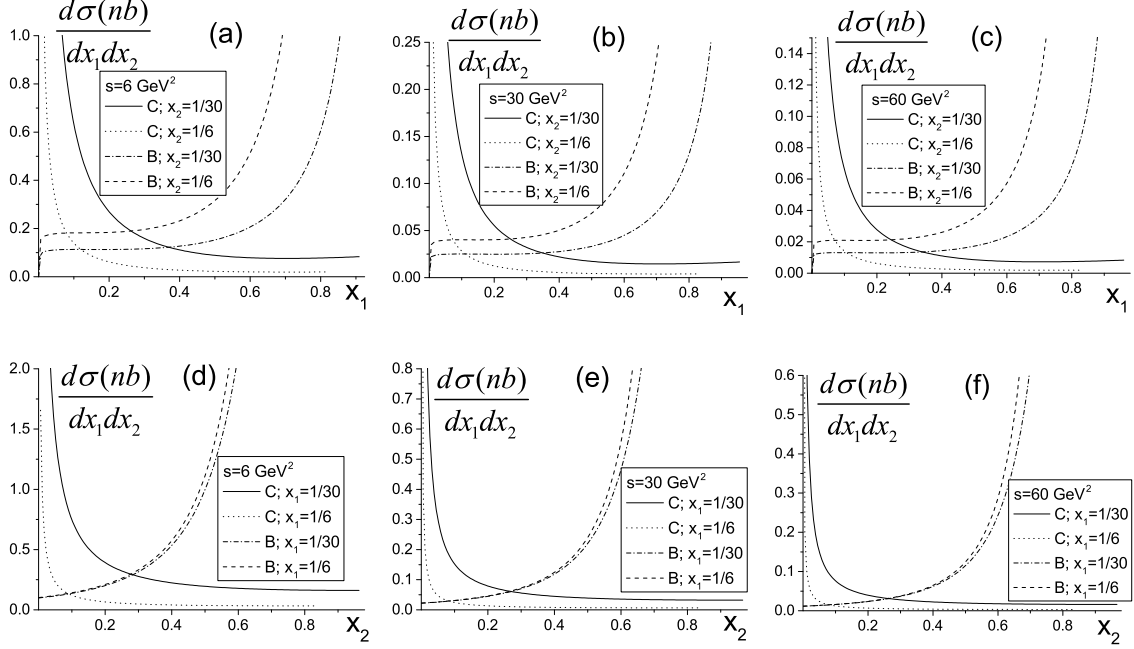


FIG. 4. Double differential cross section for the reaction $\gamma + \mu^- \rightarrow e^+ e^- + \mu^-$. In the first row it is given as a function of $x_1 = s_1/s$ for fixed values of the variable $x_2 = |u|/s$: for the Compton-type diagrams $x_2 = 1/30$ (solid line) and $x_2 = 1/6$ (dotted line), for the Borsellino diagrams $x_2 = 1/30$ (dash-dotted line) and $x_2 = 1/6$ (dashed line); and for different values of the total energy squared s : $s = 6 \text{ GeV}^2$ (a), $s = 30 \text{ GeV}^2$ (b), and $s = 60 \text{ GeV}^2$ (c); - in the second row it is given as a function of x_2 for fixed values of the variable x_1 : for the Compton-type diagrams $x_1 = 1/30$ (solid line) and $x_1 = 1/6$ (dotted line), for the Borsellino diagrams $x_1 = 1/30$ (dash-dotted line) and $x_1 = 1/6$ (dashed line), and for different values of the total energy squared s : $s = 6 \text{ GeV}^2$ (a), $s = 30 \text{ GeV}^2$ (b), and $s = 60 \text{ GeV}^2$ (c).

below. We can perform the integration over the variable u and derive an analytical result for the s_1 distribution even in the restricted phase space given by Eq. (17). In this case, the region of the variables u and s_1 is shown in Fig. 2, where the quantity s_{10} is the solution of the equation $u_0 = u_-$ and reads

$$s_{10} = \frac{(M^4 - su_0)(2M^2 - s - u_0)}{(M^2 - u_0)(s - M^2)}, \quad u_0 < \tilde{u}, \quad \tilde{u} = M \left(\frac{M^2}{\sqrt{s}} + M - \sqrt{s} \right). \quad (18)$$

Note that the solution given by Eq. (18) is the same also for the equation $u_0 = u_+$, with

$$u_0 > \tilde{u}, \quad [4m^2 < s_1 < s_{10}, \quad u_0 < u < u_+].$$

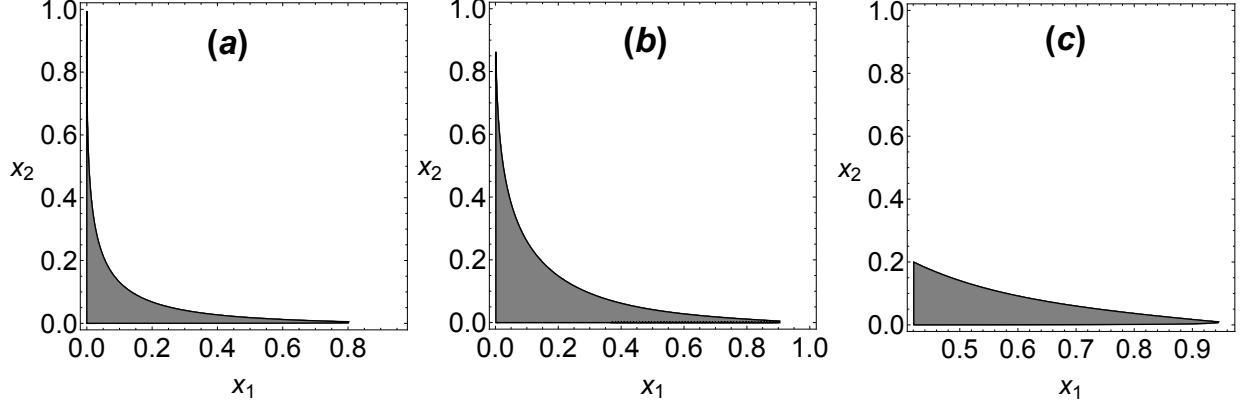


FIG. 5. Kinematical region where the Compton contribution to the double differential cross section exceeds the Borsellino contribution, at $s=30 \text{ GeV}^2$: (a) for the process $\gamma + \mu^- \rightarrow e^+ e^- + \mu^-$, (b) for the process $\gamma + e^- \rightarrow \mu^+ \mu^- + e^-$, and (c) for the processes $\gamma + e^-(\mu^-) \rightarrow \tau^+ \tau^- + e^-(\mu^-)$.

Two subregions can be delimited:

$$[4m^2 < s_1 < s_{10}, u_0 < u < u_+] ; [s_{10} < s_1 < (\sqrt{s} - M)^2, u_- < u < u_+] .$$

The event selection, under the constraint (17) (restricted phase space), decreases essentially the Borsellino contribution, whereas the Compton-type contribution decreases weakly. Their ratio

$$\tilde{R}_b^c = \frac{d\sigma_c(u > u_0)}{d\sigma_b(u > u_0)}, \quad (19)$$

in the limited phase space is shown in Fig. 6, to be compared to the ratio R_b^c .

The differential cross section of the process $\gamma + \mu^- \rightarrow e^+ e^- + \mu^-$ is illustrated in Figs. 6(a-c) taking into account all the contributions in the matrix element squared (10) and the constraint (17). This cross section is plotted as a function of the dimensionless variable x_1 , for different values of u_0 . Figure 6 shows a step decrease of this cross section, whereas s and u_0 increase. The ratio Compton-type contribution to the Borsellino one for the corresponding kinematics is shown in Figs. 6(d-f). We apply the approach developed in Ref. [33] (see also [25, 28]) to obtain the constraints on the possible values of DP parameters ϵ and $M_{A'}$ for a fixed event number N and standard deviation σ . The effective QED and DP Lagrangian [25]

$$\mathcal{L} = \mathcal{L}_{QED} + \frac{1}{2}\epsilon F^{\mu\nu} F'_{\mu\nu} - \frac{1}{4}F'^{\mu\nu} F'_{\mu\nu} + M_{A'}^2 A'^\mu A'_\mu \quad (20)$$

ensures the propagation of the fields A_μ and A'_μ and generates the interaction of the DP

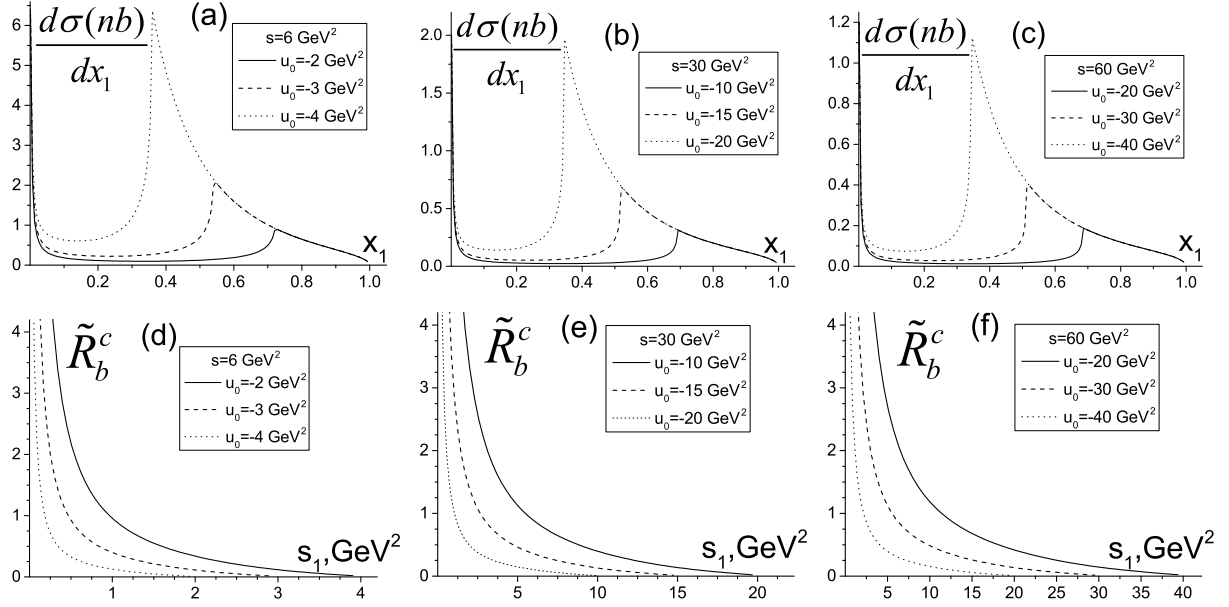


FIG. 6. Differential cross section of the process $\gamma + \mu^- \rightarrow e^+e^- + \mu^-$, as a function of the e^+e^- invariant mass squared, for the sum of the Compton-type (15) and the Borsellino (16) contributions, with the constraint (17), is shown for $s = 6 \text{ GeV}^2$ (a), $s = 30 \text{ GeV}^2$ (b), and $s = 60 \text{ GeV}^2$ (c), and for $u_0 = -2 \text{ GeV}^2$ (solid line), $u_0 = -3 \text{ GeV}^2$ (dashed line) and $u_0 = -4 \text{ GeV}^2$ (dotted line). The corresponding ratio of the Compton-type (15) to the Borsellino contributions is shown in the insets (d-f).

with the SM leptons in the form

$$e\bar{\psi}_j(x)\gamma^\mu\psi_j(x)A'_\mu, \quad j = e, \mu, \tau$$

due to the kinetic mixing effect [the second term in the rhs of Eq. (20)]. We assume that selected values of the $\ell_j^+ \ell_j^-$ invariant mass fall in the energy region

$$M_{A'} - \delta m/2 < \sqrt{s_1} < M_{A'} + \delta m/2,$$

where δm is the experimental resolution for the invariant mass, *i.e.*, the bin width containing the events of the possible signal.

The DP modifies the Compton-type matrix element by the spin-one particle Breit-Wigner propagator in such a way that its contribution into the cross section reads

$$d\sigma_{A'} = \frac{\epsilon^2 s_1 [2(s_1 - M_{A'}^2) + \epsilon^2 s_1] d\sigma_c}{D(s_1)}, \quad D(s_1) = (s_1 - M_{A'}^2)^2 + M_{A'}^2 \Gamma^2, \quad (21)$$

where the DP width Γ is defined by its decays to SM lepton pairs

$$\Gamma(\gamma' \rightarrow \ell^+\ell^-) = \epsilon^2 \frac{\alpha}{3M_{A'}^2} (M_{A'}^2 + 2m_\ell^2) \sqrt{M_{A'}^2 - 4m_\ell^2} \Theta(M_{A'} - 2m_\ell) = \epsilon^2 \Gamma_0, \quad (22)$$

where m_ℓ is the SM lepton mass and $\Theta(x)$ is the Heaviside Θ function. The term $2(s_1 - M_{A'}^2)$ in the numerator of $d\sigma_{A'}$ in Eq. (21) describes the QED-DP interference, whereas the term $\epsilon^2 s_1$ corresponds to the pure DP contribution.

In our numerical calculations, where e^+e^- or $\mu^+\mu^-$ pairs are created, we restrict ourselves to the analysis of a light DP signal with mass $M_{A'} < 1$ GeV. Then, the decay $A' \rightarrow \tau^+\tau^-$ is forbidden and, therefore, m_ℓ in (22) is the electron or the muon mass.

Bearing in mind that

$$\Gamma \ll \delta m \ll M_{A'},$$

we can apply the narrow resonance approximation and write:

$$[D(s_1)]^{-1} = \frac{\pi}{M_{A'} \epsilon^2 \Gamma_0} \delta(s_1 - M_{A'}^2).$$

Applying [28, 33]:

$$\sigma d\sigma_Q = \sqrt{N} d\sigma_{A'}, \quad (23)$$

one obtains, by integrating both sides over the bin range

$$\epsilon^2 = \frac{2\sigma}{\pi\sqrt{N}} \frac{\delta m \Gamma_0}{M_{A'}^2} \frac{d\sigma_Q(M_{A'}^2)}{d\sigma_c(M_{A'}^2)}, \quad (24)$$

where $d\sigma_Q$ is the total QED contribution.

Equation (24) defines the constraints on the parameters ϵ^2 , $M_{A'}^2$, and the number of the detected events N for a given standard deviation σ . The effect due to the QED-DP interference relative to the pure DP contribution can be easily estimated by integrating Eq. (21) at $d\sigma(s_1 = M_{A'}^2)$ over the above described bin range, giving

$$\frac{4\delta m \Gamma_0}{\pi M_{A'}^2} \ll 1.$$

These constraints are illustrated below (Figs. 7-9) at $\sigma = 2$ for the energy bin value $\delta m = 1$ MeV. In our calculations we assume that there are three channels of the DP decays into SM leptons: $A' \rightarrow e^+e^-$, $\mu^+\mu^-$, $\tau^+\tau^-$. The plots of ϵ^2 versus $M_{A'}$ for the reaction $\gamma + \mu^- \rightarrow e^+e^- + \mu^-$ are shown in Figs. 7, and 8 for $M_{A'} < 2M$ and $M_{A'} > 2M$, correspondingly. In the case of e^+e^- pair production we restrict ourselves with the DP mass

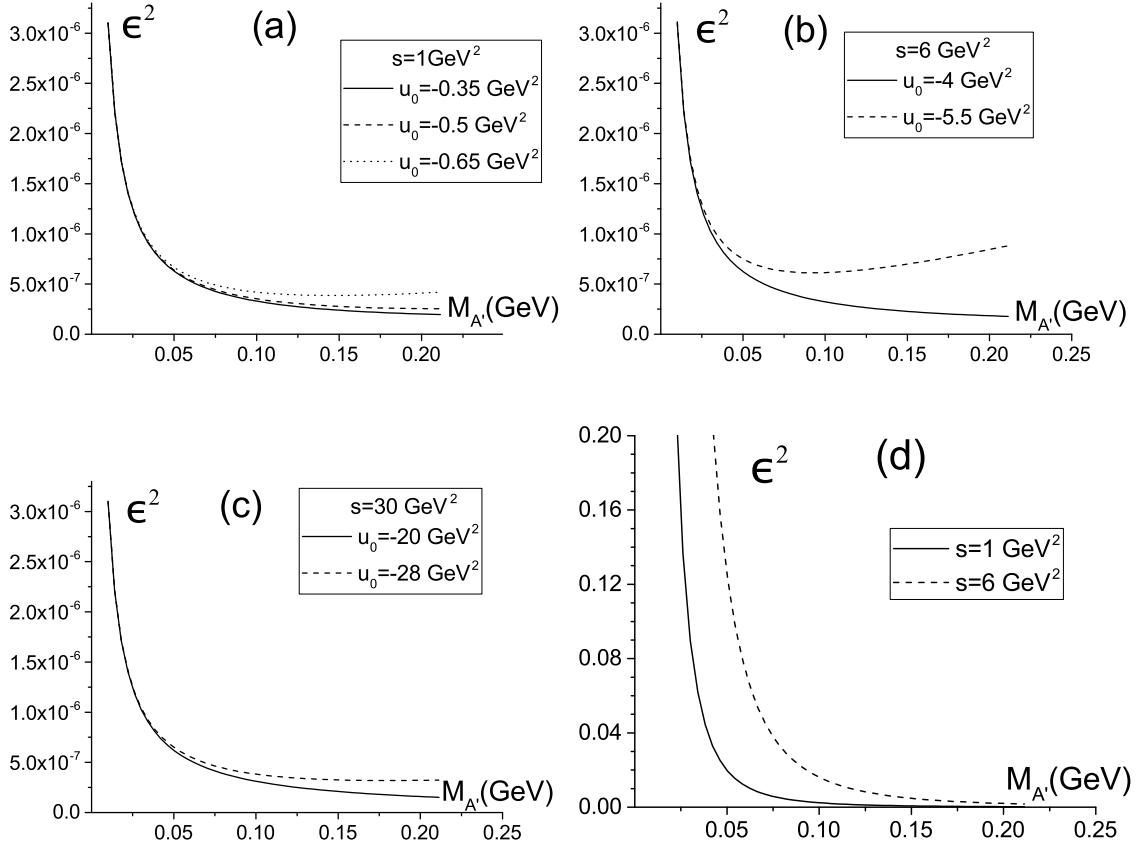


FIG. 7. Constraints on the DP parameters in terms of ϵ^2 as a function of $M_{A'}$ for the conditions: $N = 10^4$, $\sigma = 2$, and $\delta m = 1 \text{ MeV}$, in the process $\gamma + \mu^- \rightarrow e^+ e^- + \mu^-$, for $M_{A'} < 2M$, where only one channel of DP decay is allowed, for $s = 1 \text{ GeV}^2$ (a), $s = 6 \text{ GeV}^2$ (b), and $s = 30 \text{ GeV}^2$ (c). Different curves correspond to different values of u_0 , i.e., different kinematical cuts, and represent the lower limit on the DP parameters in the case of no DP event detected. Inset (d) shows the $(\epsilon^2, M_{A'})$ dependence for $s = 1 \text{ GeV}^2$ (solid line) and $s = 6 \text{ GeV}^2$ (dashed line) without kinematical cuts.

values $M_{A'} < 2m_\tau$ (m_τ is the τ lepton mass) and, therefore, take into account DP decays into $e^+ e^-$ and $\mu^+ \mu^-$ when calculating the quantity Γ_0 . The plots for the $\gamma + \mu^- \rightarrow \tau^+ \tau^- + \mu^-$ process are shown in Fig. 9. In this case, all three channels of DP decays contribute into Γ_0 .

We can conclude that the kinematical limits to reduce the contribution of the Borsellino diagrams in the cross section increase essentially the sensitivity to the DP signal and should be implemented in the experimental event selection.

The corresponding results of calculations for the reactions $\gamma + e^- \rightarrow \mu^+ \mu^- + e^-$ and

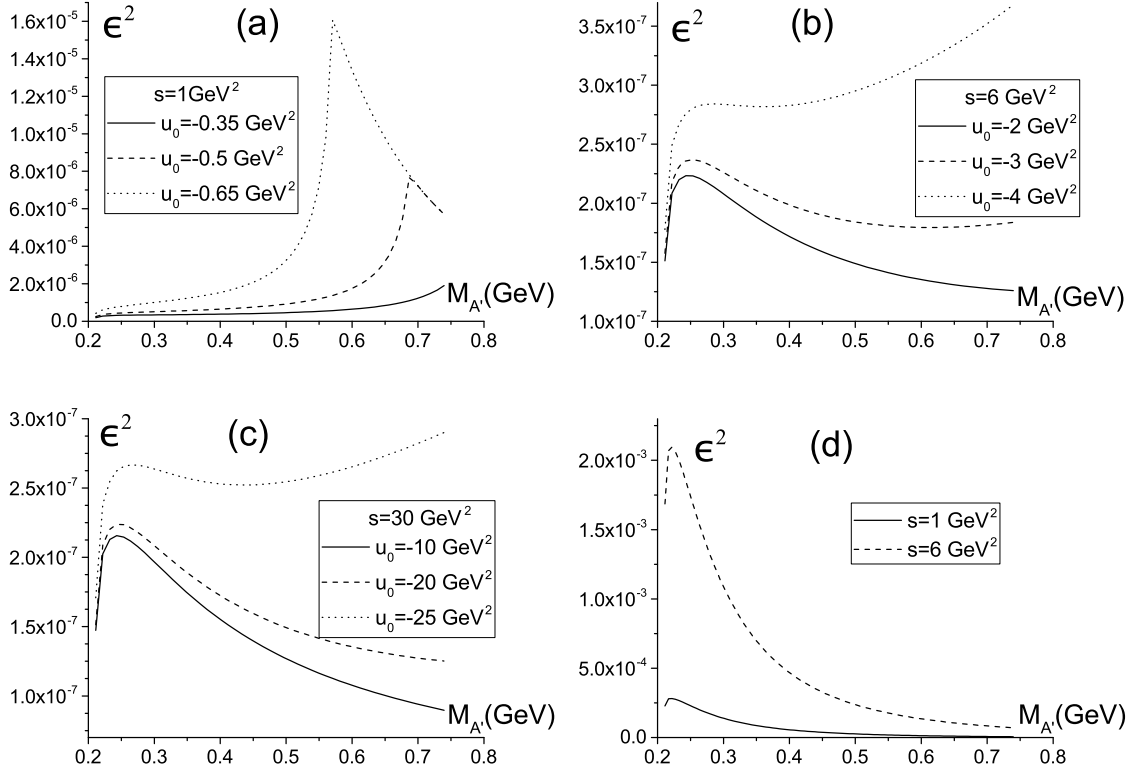


FIG. 8. The same as in Fig.7 but in the region of greater DP masses, $M_{A'} > 2M$ where two channels are open for DP decays.

$\gamma + e^- \rightarrow \tau^+ \tau^- + e^-$ are shown in Figs. 10 and 11. Again, in the case of $\mu^+ \mu^-$ production, the limit $M_{A'} < 2m_\tau$ is applied.

For every point in the $(\epsilon^2, M_{A'})$ region (at a given values of s) below curves, $\sigma < 2$ and above curves, $\sigma > 2$. If the real A' signal corresponds, at least, to three (or more) standard deviations, then the quantities ϵ^2 (at fixed $M_{A'}$), when this signal can be recorded, increase by 1.5 times (or more) as compared with the corresponding points on the curves in Figs. 7-11. To be complete, we plot also in Fig.12 the possible ϵ^2 and $M_{A'}$ bounds which can be obtained in the triplet production process $\gamma + e^- \rightarrow e^+ e^- + e^-$ for the DP masses enlarged up to 1 GeV values as compared with Ref.[33].

It is easy to see from Eq. (24) that an increase of the energy bin value δm decreases the sensitivity of the detection of the A' signal in the process (1). The reason is evident, because such an experimental device increases the QED background which is, in fact, proportional to δm and leaves unchanged the number of events due to the DP signal in the narrow A' resonance. The dependence of the sensitivity on the DP mass $M_{A'}$ is determined by the

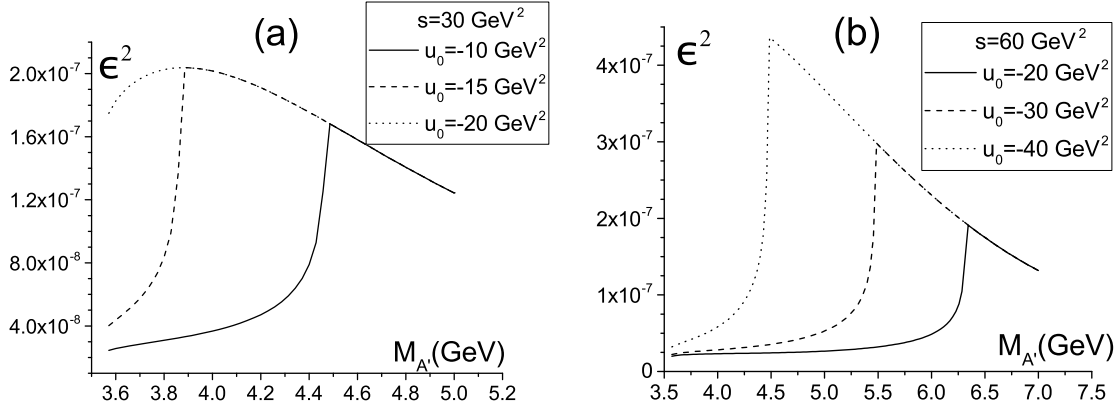


FIG. 9. ϵ^2 versus $M_{A'}$ for the reaction $\gamma + \mu^- \rightarrow \tau^+\tau^- + \mu^-$, for $s = 30 \text{ GeV}^2$ (a) and $s = 60 \text{ GeV}^2$ (b). Different curves correspond to different values of u_0 , i.e., different kinematical cuts.

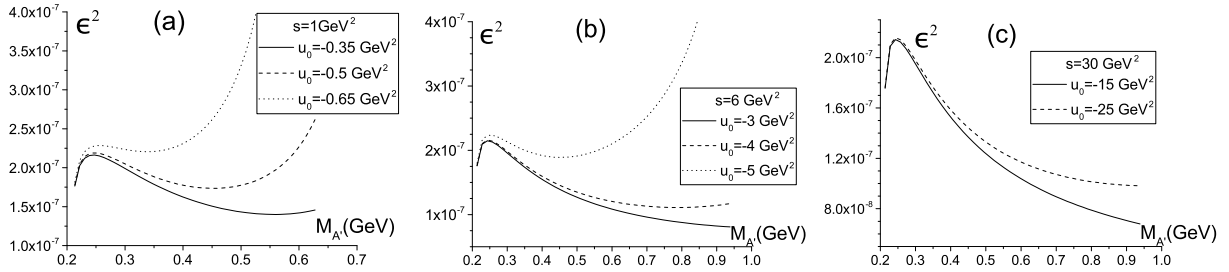


FIG. 10. The same as in Figs. 8(a-c) but for the process $\gamma + e^- \rightarrow \mu^+\mu^- + e^-$.

interplay of the $M_{A'}$ -dependences of Γ_0 , $d\sigma_Q$ and $d\sigma_c$ entering in Eq. (24). This statement takes place also if we use the exact form of $D(s_1)$ when integrating both sides of Eq. (23). Accounting for the kinematical restriction (17) increases essentially the sensitivity, due to the suppression of the QED background. To illustrate the corresponding effect, $\epsilon^2(M_{A'})$ for the reaction $\gamma + \mu^- \rightarrow e^+e^- + \mu^-$ is also plotted without the kinematical cuts.

The number of the events N in the denominator of the rhs of Eq. (24), in the frame of the described event selection, can be written with a good approximation as

$$N = \frac{2\delta m M_{A'}}{s} \frac{d\sigma_Q}{dx_1} \left(x_1 = \frac{M_{A'}^2}{s} \right) L \cdot T. \quad (25)$$

that allows one to estimate the necessary integral luminosity ($L \cdot T$) for collecting 10^4 events. Taking values for $d\sigma_Q$ in the range $10^{-31} - 10^{-34} \text{ cm}^{-2}$ (as it follows from the curves in Fig. 6) and values for $2\delta m M_{A'}/s$ in the range $10^{-3} - 10^{-1}$, one finds the interval

$$L \cdot T \approx (10^{36} - 10^{41}) \text{ cm}^{-2}$$

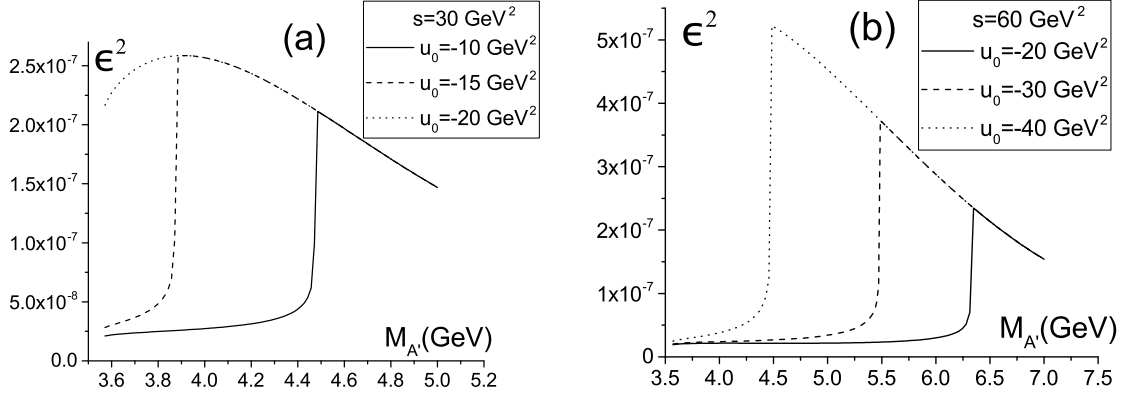


FIG. 11. The same as in Fig. 9 but for the process $\gamma + e^- \rightarrow \tau^+ \tau^- + e^-$.

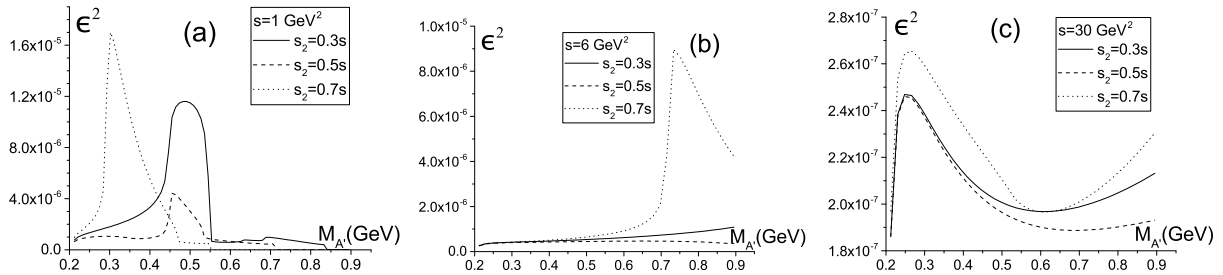


FIG. 12. The $(\epsilon^2, M_{A'})$ bounds for the DP manifestation in the process $\gamma + e^- \rightarrow e^+ e^- + e^-$ calculated by formulas of Ref. [33] but with corrected value of Γ that takes into account decay $A' \rightarrow \mu^+ \mu^-$.

at the considered values of s between 1 and 60 GeV^2 . The largest energies require the largest integral luminosity and vice versa. As concerns the radiative corrections to the QED contribution, they do not essentially change the ratio σ_Q/σ_c entering Eq. (24) and cannot essentially change the curves in Figs. 7-11.

Let us compare the constraints on the parameter ϵ estimated in our paper with the ones obtained in various experiments (see Fig. 13). The A1 Collaboration at MAMI [12] measured the mass distribution of the reconstructed e^+e^- pair in the reaction $e^- + {}^{181}\text{Ta} \rightarrow e^- + e^- + e^+ + {}^{181}\text{Ta}$. The measured limit is $\epsilon^2 < 10^{-6}$ in the following range of DP masses: $210 \text{ MeV}/c^2 < m_{e^+e^-} < 300 \text{ MeV}/c^2$ to be compared to our estimation for the ϵ^2 value in this DP mass range : $(1 - 2) \times 10^{-7}$. We suggest, instead, to measure the distribution over the invariant mass of the produced lepton pair in the reactions $\gamma + \mu^- \rightarrow e^+ + e^- + \mu^-$ and $\gamma + e^- \rightarrow \mu^+ + \mu^- + e^-$ (see Figs. 8-10). In the DP search with the KLOE detector at

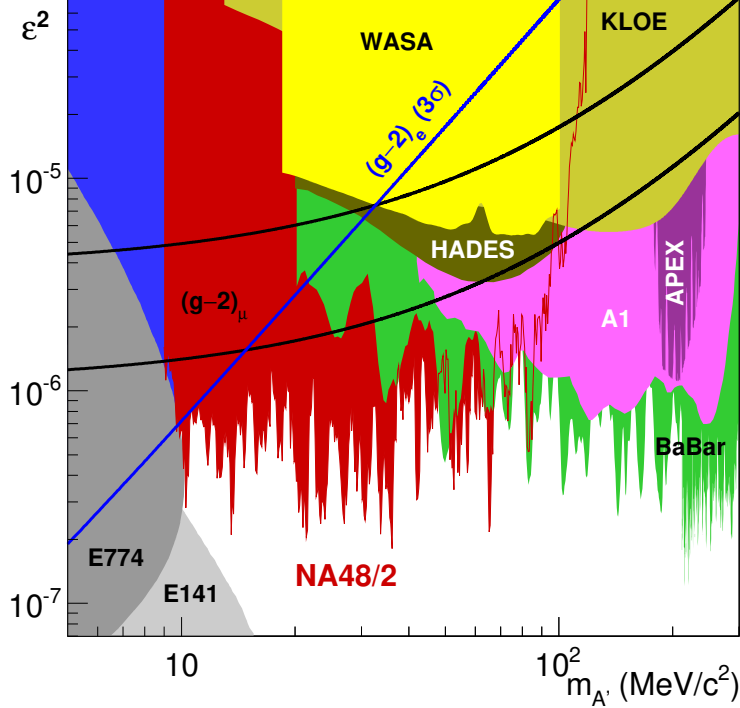


FIG. 13. The NA48/2 preliminary upper limits at 90 % CL on the mixing parameter ϵ^2 versus the DP mass $m_{A'}$ [17], compared to the other published exclusion limits from meson decay, beam dump and e^+e^- collider experiments [44]. The results obtained in Refs. [45] and [32] from the muon and electron $g - 2$ factors are also shown.

the DAΦNE e^+e^- collider [46], the authors looked for a dimuon mass peak in the reaction $e^+e^- \rightarrow \mu^+\mu^-\gamma$, corresponding to the decay $A' \rightarrow \mu^+\mu^-$. With an integrated luminosity of 239.3 pb^{-1} (5.35×10^5 events), they set a 90% C.L. upper limit for the kinetic mixing parameter ϵ^2 of 1.6×10^{-5} to 8.5×10^{-7} in the mass region $520 < m_{A'} < 980 \text{ MeV}$. Our estimation for this DP mass range is $\epsilon^2 \leq 10^{-7}$ ($\gamma + \mu^- \rightarrow e^+ + e^- + \mu^-$) and $\epsilon^2 \leq (10^{-7} - 6 \cdot 10^{-8})$ ($\gamma + e^- \rightarrow \mu^+ + \mu^- + e^-$). DP was searched as a maximum in the invariant mass distribution of e^+e^- pairs originating from the radiative decays as e.g. $\phi \rightarrow \eta e^+e^-$ in the experiment [47]. Only an upper limit was set with 90% C.L. on $\epsilon^2 < 1.7 \times 10^{-5}$ for $30 < M_{A'} < 400 \text{ MeV}$ and $\epsilon^2 < 8 \times 10^{-6}$ for the subregion $50 < M_{A'} < 210 \text{ MeV}$. Our results are competitive also in these conditions: $\epsilon^2 \leq 10^{-7}$ ($\gamma + \mu^- \rightarrow e^+ + e^- + \mu^-$).

Some published exclusion limits on the DP parameter space from meson decay, beam dump and e^+e^- collider experiments [44] are presented in Fig. 13, readapted from Fig. 6 in Ref. [17].

Let us summarize the advantages of the photoproduction reactions with different lepton flavors in the final state

1. In order to obtain the master bidimensional distribution (s_1, u) , it is sufficient to measure only the ℓ_i particle 4-momentum. The master distribution does not contain the interference between the Compton-type and the Borsellino diagrams, which simplifies essentially the theoretical analysis.
2. In order to suppress the background due to the Borsellino contribution it is sufficient to set a cut only in one invariant variable (if all final flavors are the same, one needs a cut in two variables).
3. The DP physical events are accumulated in a wide region of invariant variables, allowing one to reduce the necessary integral luminosity. In the case of triplet photoproduction, besides the two cuts on invariant variables mentioned above, the events must be selected at a fixed value of one (from two final) $e^+ e^-$ pair.

IV. CONCLUSION

We investigated the direct detection of dark photon, one of the new particles that may possibly shed light on the nature and on the interaction of dark matter. The DP is mixed with the ordinary photon due to the effect of the kinetic mixing and it can, therefore, interact with the SM leptons. It is characterized by a mass $M_{A'}$ and a small parameter ϵ describing the coupling strength relative the electric charge e .

We analyzed a possible way to detect a DP signal when its mass lies in the range between few MeV and few GeV. This mass region is presently accessible at the existing accelerators. The idea is to scan the distribution of the invariant mass squared of the $\ell_j^+ \ell_j^-$ system, s_1 , in the reactions $\gamma + \ell_i \rightarrow \ell_j^+ \ell_j^- + \ell_i$ with $i \neq j$ and $i = e, \mu$; $j = e, \mu, \tau$, where few tens MeV photons collide with high-energy electron or muon beams. Because of the interaction with SM leptons, DP appears as a narrow resonance in the $\ell_j^+ \ell_j^-$ -system over a background, and modifies the Compton-type diagrams by the Breit-Wigner term. Choosing processes with $i \neq j$ one avoids the ambiguity of the measurements arising from the final particle identity.

First, we calculated the double differential cross section with respect to the variables s_1 , and u and then derived the s_1 distribution after integration over the variable u . Note that to

measure such double differential cross section it is sufficient to measure the four-momentum of the final lepton ℓ_i .

The advantage of this reaction is that the background is of a pure QED origin and can be calculated exactly with the necessary precision.

In the case when all kinematically possible values of the variable u are taken into account, a large QED background arises due to the contribution of the Borsellino diagrams, as illustrated in Fig. 3. To suppress this background, we analyzed the (s_1, u) distribution and identified the kinematical regions where the contribution of the Compton-type diagrams exceed the Borsellino ones (see Fig. 4.). The background contribution increases when the variables s_1 and u decrease, whereas the DP signal has just the opposite behavior. Therefore we applied different cuts ($u > u_0$) to exclude the range of large values of $|u|$ (see Figs. 5 and 6).

Selecting the restricted (s_1, u) region, we estimated the constraints on the possible values of the parameters ϵ^2 and $M_{A'}$ for a given number of the detected events, $N = 10^4$, and standard deviation $\sigma = 2$ for all considered reactions (see Figs. 7 -11). Our results suggest that a convenient bin width containing all the events of the possible DP signal near $s_1 = M_{A'}$ could be $\delta m = 1$ MeV. Equation (24) determines the relation between ϵ^2 and $M_{A'}$ as a function of the parameters N , σ and δm .

V. ACKNOWLEDGMENTS

Two of us (N.P.M. and M.I.K) acknowledge the hospitality of IRFU/DPhN, under the Paris-Saclay grant AAP-P2I-DARKPHI. This work was partially supported by the Ministry of Education and Science of Ukraine (project n. 0118U002031). The research was conducted in the scope of the IDEATE International Research Project (IRP). This work was partially supported by the ERASMUS+ program (code F PARIS 011).

VI. APPENDIX

To obtain the s_1 distribution it is convenient to define the quantity

$$\int \frac{d\sigma_i}{ds_1 du} du \equiv F_i(s, s_1, u), \quad i = b, c.$$

Then we have;

$$\begin{aligned}
F_b(s, s_1, u) = & \frac{\alpha^3}{\pi(s - M^2)} \left\{ \frac{\sqrt{s_1 - 4m^2}}{\sqrt{s_1}} \left[\frac{2(4m^2 + s_1)M^2}{(M^2 - s)(-2M^2 + s + u - s_1)s_1} + \right. \right. \\
& \frac{8(M^2 - s)(m^2 + 2s_1)}{3(-2M^2 + s + u)^3} + \frac{4[(M^2 - s + s_1)m^2 + 2s_1^2]}{(-2M^2 + s + u)^2s_1} + \\
& \frac{2}{(M^2 - s)(-2M^2 + s + u)s_1^2} [2(2M^4 - 4(s - s_1)M^2 + 2s^2 + s_1^2 - 2ss_1)m^2 + \\
& \left. \left. s_1[M^4 - 2(s - 2s_1)M^2 + s^2 + 2s_1^2] \right] - \ln \left(\frac{\sqrt{s_1} + \sqrt{s_1 - 4m^2}}{2m} \right) \times \right. \\
& \left[\frac{4(-8m^4 + 4s_1m^2 + s_1^2)M^2}{(M^2 - s)(-2M^2 + s + u - s_1)s_1^2} + \frac{8(M^2 - s)(-4m^4 + 6s_1m^2 + s_1^2)}{3(-2M^2 + s + u)^3s_1} + \right. \\
& \left. + \frac{4[-4(M^2 - s + s_1)m^4 + 2s_1(M^2 - s + 3s_1)m^2 + s_1^3]}{(-2M^2 + s + u)^2s_1^2} + \right. \\
& \left. \frac{4}{(M^2 - s)(-2M^2 + s + u)s_1^3} [s_1^2[(M^2 - s)^2 + s_1(2M^2 + s_1)] + \right. \\
& \left. \left. 2m^2(2m^2 - s_1)[2M^4 - 4(s - s_1)M^2 + 2s^2 + s_1^2 - 2ss_1] \right] + \right. \\
& \left. \frac{2 \ln(-2M^2 + s + u)}{(M^2 - s)s_1^4} \left[-\sqrt{s_1}\sqrt{s_1 - 4m^2} \times \right. \right. \\
& \left. \left. [2[2M^4 + (6s_1 - 4s)M^2 + 2s^2 + s_1^2 - 2ss_1]m^2 + s_1[M^4 + (5s_1 - 2s)M^2 + s(s - s_1)]] \right] - \right. \\
& \left. 2 \ln \left(\frac{\sqrt{s_1} + \sqrt{s_1 - 4m^2}}{2m} \right) [2m^2(2m^2 - s_1)[2M^4 + (6s_1 - 4s)M^2 + 2s^2 + s_1^2 - 2ss_1] + \right. \\
& \left. s_1^2[M^4 + (3s_1 - 2s)M^2 + s(s - s_1)] + \right. \\
& \left. \frac{\ln(-2M^2 + s + u - s_1)}{(M^2 - s)s_1^4} \left[2 \ln \left(\frac{\sqrt{s_1} + \sqrt{s_1 - 4m^2}}{2m} \right) (8m^4 - 4s_1m^2 - s_1^2) \times \right. \right. \\
& \left. \left. [2M^4 + (6s_1 - 4s)M^2 + 2s^2 + s_1^2 - 2ss_1] + \sqrt{s_1}\sqrt{s_1 - 4m^2} \times \right. \right. \\
& \left. \left. [4[2M^4 + (6s_1 - 4s)M^2 + 2s^2 + s_1^2 - 2ss_1]m^2 + \right. \right. \\
& \left. \left. \left. s_1[2M^4 + (10s_1 - 4s)M^2 + 2s^2 + s_1^2 - 2ss_1] \right] \right] \right\}, \\
F_c(s, s_1, u) = & -\frac{\alpha^3\sqrt{s_1 - 4m^2}(2m^2 + s_1)}{3\pi s_1^{5/2}(M^2 - s)^4} \left[-\frac{1}{2}u^2(M^2 - s) - \frac{2M^2(2M^2 + s_1)(M^2 - s)^2}{M^2 - u} + \right.
\end{aligned}$$

$$\left. [3M^4 + M^2(6s - 2s_1) - s^2 - 2s_1^2 + 2ss_1](M^2 - s) \log(u - M^2) + u(M^4 - 5M^2s - 2ss_1) \right].$$

The single s_1 distribution [Eqs. (15 and 16)] is the difference

$$F_i(s, s_1, u_+) - F_i(s, s_1, u_-),$$

where the analytical form of the s_1 -distribution for the restricted phase space defined by Eq. (17), is given as

$$F_i(s, s_1, u = u_+) - F_i(s, s_1, u = u_0), \quad i = b, c.$$

This expression is valid if $s_1 < s_{10}$, where s_{10} is the solution of the equation $u_- = u_0$ (see Fig. 2).

-
- [1] Y. Fukuda *et al.* (Super-Kamiokande Collaboration), Phys. Rev. Lett. **81**, 1562 (1998), arXiv:hep-ex/9807003 [hep-ex].
 - [2] F. Jegerlehner and A. Nyffeler, Phys. Rep. **477**, 1 (2009), arXiv:0902.3360 [hep-ph].
 - [3] D. Wackerroth, in *54th Rencontres de Moriond on QCD and High Energy Interactions (Moriond QCD 2019) La Thuile, Italy, March 23-30, 2019* (2019) arXiv:1906.09138 [hep-ph].
 - [4] J. Hewett *et al.* (2012) arXiv:1205.2671 [hep-ex].
 - [5] Essig, R. and Jaros, J.A. and Wester, W., in *Proceedings, 2013 Community Summer Study on the Future of U.S. Particle Physics: Snowmass on the Mississippi (CSS2013): Minneapolis, MN, USA, July 29-August 6, 2013* (2013) arXiv:1311.0029 [hep-ph].
 - [6] A. Soffer, *Proceedings, 13th Conference on Flavor Physics and CP Violation (FPCP 2015): Nagoya, Japan, May 25-29, 2015*, PoS **FPCP2015**, 025 (2015), arXiv:1507.02330 [hep-ex].
 - [7] J. Alexander *et al.* (2016) arXiv:1608.08632 [hep-ph].
 - [8] B. Holdom, Phys. Lett. **B178**, 65 (1986).
 - [9] R. Essig, P. Schuster, N. Toro, and B. Wojtsekhowski, JHEP **02**, 009 (2011), arXiv:1001.2557 [hep-ph].
 - [10] S. Abrahamyan *et al.* (APEX), Phys. Rev. Lett. **107**, 191804 (2011), arXiv:1108.2750 [hep-ex].
 - [11] M. Freytsis, G. Ovanesyan, and J. Thaler, JHEP **01**, 111 (2010), arXiv:0909.2862 [hep-ph].
 - [12] H. Merkel *et al.* (A1), Phys. Rev. Lett. **106**, 251802 (2011), arXiv:1101.4091 [nucl-ex].

- [13] C. Bravo (HPS), in *Meeting of the Division of Particles and Fields of the American Physical Society (DPF2019) Boston, Massachusetts, July 29-August 2, 2019* (2019) arXiv:1910.04886 [hep-ex].
- [14] E. Frlez *et al.*, Phys. Rev. Lett. **93**, 181804 (2004), arXiv:hep-ex/0312029 [hep-ex].
- [15] X. Wang, X. Chen, Q. Zeng, W. Jiang, R. Wang, and B. Zhang, (2013), arXiv:1312.3144 [hep-ph].
- [16] P. Moskal *et al.* (WASA-at-COSY), in *Proceedings, 49th Rencontres de Moriond on QCD and High Energy Interactions: La Thuile, Italy, March 22-29, 2014* (2014) pp. 237–242, arXiv:1406.5738 [nucl-ex].
- [17] E. Goudzovski (NA48/2), *Proceedings, Dark Matter, Hadron Physics and Fusion Physics (DHF2014): Messina, Italy, September 24-26, 2014*, EPJ Web Conf. **96**, 01017 (2015), arXiv:1412.8053 [hep-ex].
- [18] G. Agakishiev *et al.* (HADES), Phys. Lett. **B731**, 265 (2014), arXiv:1311.0216 [hep-ex].
- [19] S. Andreas, *Proceedings, Dark Forces at Accelerators (DARK2012): Frascati, Italy, October 16-19, 2012*, Frascati Phys. Ser. **56**, 23 (2012), arXiv:1212.4520 [hep-ph].
- [20] E. Izaguirre, G. Krnjaic, P. Schuster, and N. Toro, Phys. Rev. **D90**, 014052 (2014), arXiv:1403.6826 [hep-ph].
- [21] G. Inguglia (Belle II), in *33rd Rencontres de Physique de La Valle d’Aoste (LaThuile 2019) La Thuile, Aosta, Italy, March 10-16, 2019* (2019) arXiv:1906.09566 [hep-ex].
- [22] J. P. Lees *et al.* (BaBar), Phys. Rev. Lett. **119**, 131804 (2017), arXiv:1702.03327 [hep-ex].
- [23] B. Wojtsekhowski, *Positrons at Jefferson Lab. Proceedings, International Workshop, JPOS 09, Newport News, USA, March 25-27, 2009*, AIP Conf. Proc. **1160**, 149 (2009), arXiv:0906.5265 [hep-ex].
- [24] J. Jiang, C.-Y. Li, S.-Y. Li, S. D. Pathak, Z.-G. Si, and X.-H. Yang, (2019), arXiv:1910.07161 [hep-ph].
- [25] J. D. Bjorken, R. Essig, P. Schuster, and N. Toro, Phys. Rev. **D80**, 075018 (2009), arXiv:0906.0580 [hep-ph].
- [26] T. Beranek, H. Merkel, and M. Vanderhaeghen, Phys. Rev. **D88**, 015032 (2013), arXiv:1303.2540 [hep-ph].
- [27] T. Beranek and M. Vanderhaeghen, Phys. Rev. **D89**, 055006 (2014), arXiv:1311.5104 [hep-ph].
- [28] C.-W. Chiang and P.-Y. Tseng, Phys. Lett. **B767**, 289 (2017), arXiv:1612.06985 [hep-ph].

- [29] H. An, M. Pospelov, J. Pradler, and A. Ritz, Phys. Lett. **B747**, 331 (2015), arXiv:1412.8378 [hep-ph].
- [30] H. Park, Phys. Rev. Lett. **119**, 081801 (2017), arXiv:1705.02470 [hep-ph].
- [31] S.-F. Ge and I. M. Shoemaker, JHEP **11**, 066 (2018), arXiv:1710.10889 [hep-ph].
- [32] M. Pospelov, Phys. Rev. **D80**, 095002 (2009), arXiv:0811.1030 [hep-ph].
- [33] G. I. Gakh, M. I. Konchatnij, and N. P. Merenkov, J. Exp. Theor. Phys. **127**, 279 (2018), [Zh. Eksp. Teor. Fiz.154,no.2,326(2018)].
- [34] X. Chen, Z. Hu, and Y. Wu, (2020), arXiv:2001.04382 [hep-ph].
- [35] J. Jaeckel and A. Ringwald, Ann. Rev. Nucl. Part. Sci. **60**, 405 (2010), arXiv:1002.0329 [hep-ph].
- [36] G. G. Raffelt, *Stars as laboratories for fundamental physics* (1996).
- [37] H. An, M. Pospelov, and J. Pradler, Phys. Lett. **B725**, 190 (2013), arXiv:1302.3884 [hep-ph].
- [38] G. Pignol, B. Clement, M. Guigue, D. Rebreyend, and B. Voirin, (2015), arXiv:1507.06875 [astro-ph.CO].
- [39] J. L. Feng, J. Smolinsky, and P. Tanedo, Phys. Rev. **D93**, 115036 (2016), [Erratum: Phys. Rev.D96,no.9,099903(2017)], arXiv:1602.01465 [hep-ph].
- [40] M. Battaglieri *et al.*, in *U.S. Cosmic Visions: New Ideas in Dark Matter College Park, MD, USA, March 23-25, 2017* (2017) arXiv:1707.04591 [hep-ph].
- [41] B. Byckling and K. Kajantie, *Particle kinematics*, Wiley interscience publication (John Wiley and Sons, 1972).
- [42] W. H. Furry, Phys. Rev. **51**, 125 (1937).
- [43] V. F. Boldyshev, E. A. Vinokurov, N. P. Merenkov, and Yu. P. Peresunko, Phys. Part. Nucl. **25**, 292 (1994).
- [44] J. P. Lees *et al.* (BaBar), Phys. Rev. Lett. **113**, 201801 (2014), arXiv:1406.2980 [hep-ex].
- [45] H. Davoudiasl, H.-S. Lee, and W. J. Marciano, Phys. Rev. **D89**, 095006 (2014), arXiv:1402.3620 [hep-ph].
- [46] D. Babusci *et al.* (KLOE-2), Phys. Lett. **B736**, 459 (2014), arXiv:1404.7772 [hep-ex].
- [47] P. Moskal *et al.* (KLOE, KLOE-2), in *Proceedings, 48th Rencontres de Moriond on QCD and High Energy Interactions: La Thuile, Italy, March 9-16, 2013* (2013) pp. 275–278, arXiv:1306.5740 [hep-ex].